Multi-scale numerical modeling of the multi-pass rolling texture evolution by using crystal plasticity and finite element method

BYRSKA-WÓJCIK Dorota[1,a *], WIERZBANOWSKI Krzysztof[1,b], WRÓBEL Mirosław[1,c] and BŁONIARZ Remigiusz[1,d]

[1]AGH University of Krakow, al. Mickiewicza 30, 30-059 Krakow, Poland

[a]byrska@agh.edu.pl, [b]Krzysztof.Wierzbanowski@fis.agh.edu.pl, [c]mwrobel@agh.edu.pl, [d]bloniarz@agh.edu.pl

Keywords: Multiscale Model, Multi-Pass, Finite Element Method, Crystal Plasticity, Asymmetric Rolling, Aluminum, Texture, Product Homogeneity

Abstract. The finite element method (FEM) combined with the crystal plasticity (CP) model was used to predict crystallographic texture evolution during multi-pass asymmetric rolling of the polycrystalline aluminum with tilted entry into the rolling gap. The FEM macro-scale model of the rolling process with various asymmetry was performed using Abaqus commercial software. The asymmetry was introduced by difference in the diameters of cooperating rolls and various tilt angles of the rolled bar entry into the rolling gap. Predicted stress distribution over sample volume was used as the boundary conditions in the crystal plasticity meso-scale model of the plastic deformation. The CP meso-scale model developed by Leffers and Wierzbanowski [1], [2] was used as a post-processing procedure. The predicted evolution of the rolling texture distribution on the rolled bar thickness turned out to be in good agreement with that measured for specimens rolled with the same parameters as the ones used for modeling. Impact of the rolling parameters on the texture evolution was found.

Introduction

Rolling is one of the most used processes in metal forming due to its simplicity and economic aspects. Traditionally, symmetric rolling has been used. However, it has been shown that the use of appropriate and controlled asymmetry can bring tangible benefits. Thus, in this way it is possible to significantly homogenize the microstructure and crystallographic texture (shortly texture) distribution throughout the product thickness. Therefore, asymmetric rolling of various metals has been recently studied, and a vast literature on this subject is available (e.g., [3]–[5]). According to the Web of Science, approximately 160 publications on this topic were published annually in 2022 and 2023, and during this period the average annual number of citations was over 5,000. The texture effect has been depicted in numerous papers (e.g. [2], [4], [6]–[9]) and improvement in texture gradient by tilt rolling has been patented [10]. The influence of rolling asymmetry on mechanical properties and microstructure has also been frequently characterized (e.g. [3], [6], [7], [11], [12]). However, most of these papers focused on experimental studies, and numerical analysis is usually limited to single-pass rolling processes and often involve only the horizontal introduction of the rolled strip into the rolling gap. The present paper is devoted to development of a multi-scale numerical model of multi-pass asymmetric rolling for which the asymmetry is caused by both a difference in the diameters of cooperating rolls and various tilt angles of the rolled bar entry into rolling gap.

Experiment and material

The 6-pass rolling process for pure aluminum was done in laboratory conditions using a 4-high rolling mill. The asymmetry was introduced by a difference in rolls diameters ($\boldsymbol{d_1}$ and $\boldsymbol{d_2}$ in Fig. 1) and by tilting the rolled bar into rolling gap (the tilt angle $\boldsymbol{\alpha}$ in Fig. 1). The diameter of the upper roll was 100 mm while the diameter of the lower one was equal to 100 or 120 mm. Three values of the tilt angle were used, i.e., $\boldsymbol{\alpha} = \mathbf{0}°$, $\mathbf{30}°$ or $-\mathbf{30}°$ where the positive sign refers to the tilt towards the smaller, upper roll and negative one towards the bigger, lower one (see Fig. 1). The initial sample thickness was 5 mm. The roll distance set for each pass (see table 1) did not change significantly during rolling.

Table 1. Distance between rolls in each pass of rolling.

Pass number	1	2	3	4	5	6
Distance between rolls [mm]	4.2	3.51	2.8	2.09	1.43	0.99

Multi-scale numerical model

The developed model combines a macro-scale finite element (FE) description with a meso-scale crystal plasticity (CP) approach. Thus, the stress/strains fields predicted by the macro-scale simulations of multi-stage asymmetric rolling with the parameters used in the experiment were applied to determine the boundary conditions for the meso-scale CP numerical model of plastic deformation. This way it was possible to calculate the rolling texture evolution. The scheme of the multi-scale approach can be seen in Fig. 1.

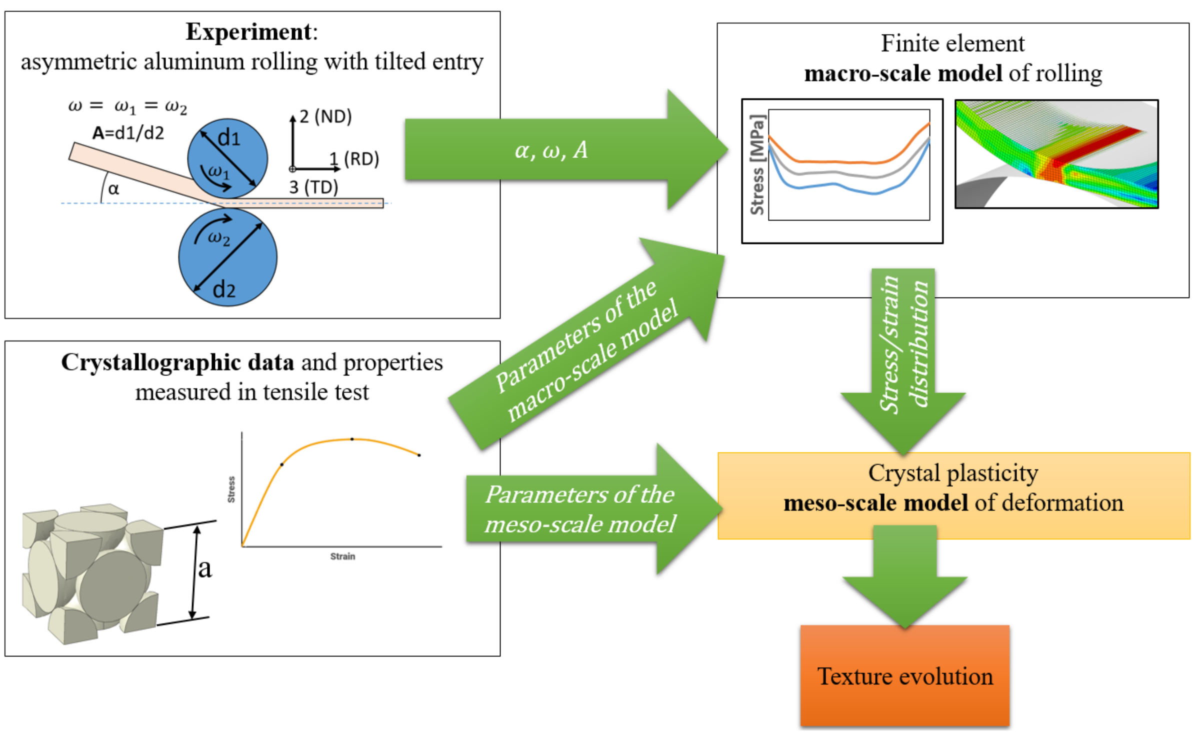

Fig. 1. The idea of the multi-scale approach used.

Macro-scale model

The three-dimensional macro-scale model of rolling was prepared by using commercial Abaqus software. The reference sets, rolling geometry and finite element mesh are presented in Fig. 2. The mesh consisted of 59 004 elements of type C3D8R (linear brick element, with integration reduced to one point).

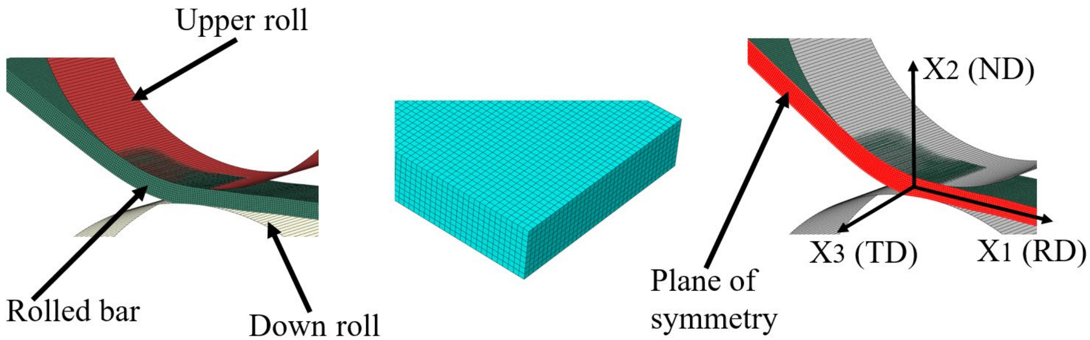

Fig. 2. Geometry of the Abaqus model (on the left), FE mesh (in the middle) and plane of symmetry (on the right).

Modelling of the multi-stage process (6 passes) requires transferring the deformed mesh and resulting stresses and strains fields after each pass to the initial conditions of the next one. Rolls are simulated as rigid body with constant angular velocity. No lubrication during rolling experiment was applied, thus the friction coefficient between the rolls and rolled bar was taken as equal to 0.3. The mirror symmetry at the center of the rolled bar along the rolling direction was assumed (symmetry plane perpendicular to $X_3 = \text{TD}$, see Fig. 2), thus only half of bar width was taken into account. All variants' simulations were performed in ACK Cyfronet using supercomputer Ares, but calculations can be also done on standard PC computer. The estimated time of calculations for one variant of a 6-pass rolling should not be longer than few days, thus this model could be recommended for usage in industry as tool for rolling asymmetry optimization.

Meso-scale model

The utilized meso-scale model was developed by Leffers and Wierzbanowski [1], [2], [13]. It is based on crystal plasticity theory. The relationship between the stress and strain in the sample and in the grain is the following:

$$\dot{\sigma}_{ij} = \dot{\Sigma}_{ij} + \alpha G\left(\dot{E}_{ij}^{p} - \dot{\epsilon}_{ij}^{p}\right), \tag{1}$$

where σ_{ij} and ϵ_{ij}^{p} are the local stress and plastic strain of a grain and Σ_{ij} and $\mathrm{E}_{\mathrm{ij}}^{\mathrm{p}}$ are their global equivalents. G is a shear modulus of the material, and α is the elasto-plastic accommodation parameter. The Einstein summation notation is used in this and following formulas. In a face-centered-cubic (fcc) metal with a high stacking fault energy (like aluminum) deformed at room temperature, crystallographic slip of the perfect dislocation with Burgers vector of (*a*/2) <110> on the {111} planes is dominant (a – is the lattice parameter). According to Schmid's law [14], slip occurs when the resolved shear stress τ reaches the critical value τ_{cr}:

$$\tau = m_i n_j \sigma_{ij} = \tau_{cr}, \tag{2}$$

where m is the slip direction and n is the slip plane normal vector (in our case <110> and <111> vectors, respectively). The value of critical resolved shear stress τ_{cr} increases with deformation due to the material hardening which is anisotropic. Thus, hardening of the slip system i depends on shear glides on other slip systems j ($d\gamma^j$):

$$d\tau_{cr}^{i} = H^{ij} d\gamma^{j}, \tag{3}$$

where H^{ij} is the strain hardening matrix.

The total plastic strain of a grain I is the sum of glides on the active slip systems (s) combination:

$$\Delta\epsilon_{ij}^{p(I)} = \sum_s \left[\frac{1}{2}\left(m_i^s n_j^s + m_j^s n_i^s\right)\delta\gamma^s\right]. \tag{4}$$

Thus, the plastic strain increment of the polycrystalline sample can be expressed as the average of its grains' strains:

$$\Delta E_{ij}^{p} = \frac{1}{V_0}\Delta\epsilon_{ij}^{p(I)} V^I, \tag{5}$$

where V_0 is the sample volume and V^I is the volume of the grain I.

Rotation of the grain lattice can be calculated by:

$$\delta\omega_{ij} = -\frac{1}{2}\left(m_i n_j - m_j n_i\right)\delta\gamma. \tag{6}$$

This rotation results in an increase in the share of preferential crystallographic orientations (i.e., in development of the crystallographic texture). During simulation the texture developed from 1000 initially randomly oriented grains. It was presented as the Orientation Distribution Function (ODF) in the Euler orientation space. Bunge convention of the Euler angles rotations was used [15]. Description of the mathematical details of the model used can be found elsewhere [1], [13].

Values of the stress tensor components evolution obtained from the macro-scale FEM model for movement of the selected integration point through the deformation zone in 6 passes were introduced in the equation (1). The first rolling pass evolution of the stress components can be seen in Tables 3 and 4, as an example. The final textures both models predicted and measured are shown in Tables 3 and 4 as the $\Phi_2 = 0°$ ODF sections. The m3m (O_h) cubic symmetry of the crystal and no sample symmetry were assumed during ODF calculations.

Results

The von Mises stress field and selected stress field components for the first pass of symmetric and asymmetric rolling can be seen in Table 2. Changes in selected stress components on the rolled bar lower surface in the rolling gap of the first pass can be also seen in Tables 3 and 4. They clearly show a trend typical for all rolling passes. The rolling asymmetry effect on the stress field isclearly visible.

Differences in the evolution of the stress and strain fields caused by rolling asymmetry result in differences in the development of the crystallographic texture, as expected. One can see this in the ODFs cross sections from Tables 3 and 4 as a value of the maxima shift along Φ. This effect is visible for both simulated and measured textures. Although quantitative differences between these results are visible, the qualitative nature is the same. Considering the simplicity of the model used to simulate the texture development, the simulation results can be considered satisfactory.

Table 2. Stress distribution for the first pass of the rolling.

Rolling variant	Mises stress [MPa]  0 11 22 32 43 54 65 76 87 98 108 119 130	σ_{12} [MPa]  -71 -59 -47 -36 -24 -12 0 12 24 35 47 59 71	σ_{22} [MPa] 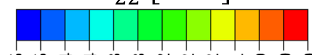 -285 -255 -224 -194 -163 -133 -102 -72 -42 -11 19 50 80
$A = 1.0$ $\alpha = 0°$	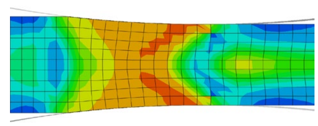	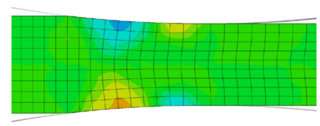	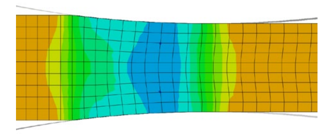
$A = 1.0$ $\alpha = 30°$	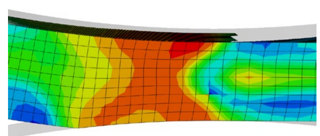	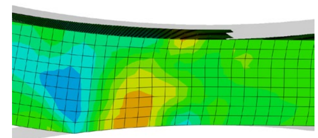	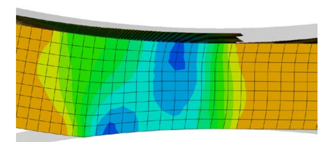
$A = 1.2$ $\alpha = 0°$	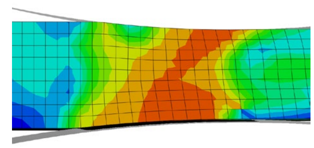	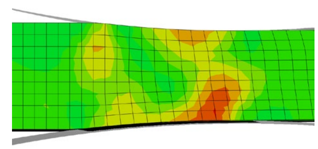	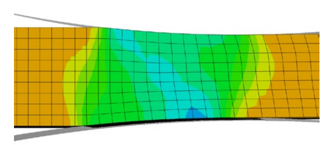
$A = 1.2$ $\alpha = 30°$	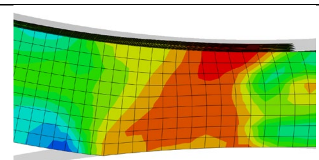	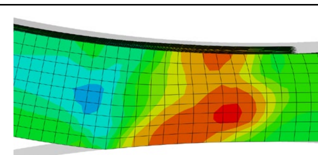	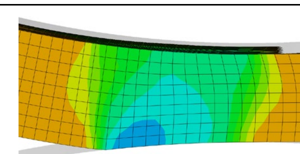
$A = 1.2$ $\alpha = -30°$	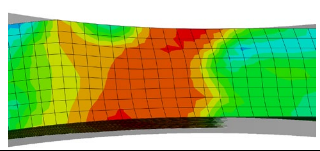	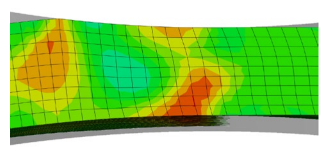	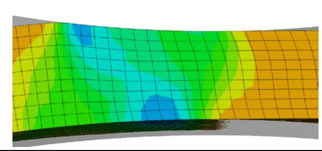

Significant changes in the rolled material flow due to rolling asymmetry can also be clearly discerned in the FE mesh deformation. Selected examples for the third pass of symmetric ($A = 1.0$), and asymmetric ($A = 1.2$) rolling with different tilt angle values can be seen in Fig. 3. For symmetric rolling (Fig. 3a), the two-fold symmetry axis parallel to RD and lying in the thickness center of the rolled strip is visible. The two-fold symmetry axis parallel to ND attached to the half thickness plane describe symmetry of the upper and lower part of the bar rolled with $A = 1.0$ and $\alpha = 30°$ (Fig. 3b). The lack of this type of symmetry is visible for the remaining cases. However, differences in the way the material flows on the rolling bar thickness are minimized for cases shown in Figs. 3c and 3e.

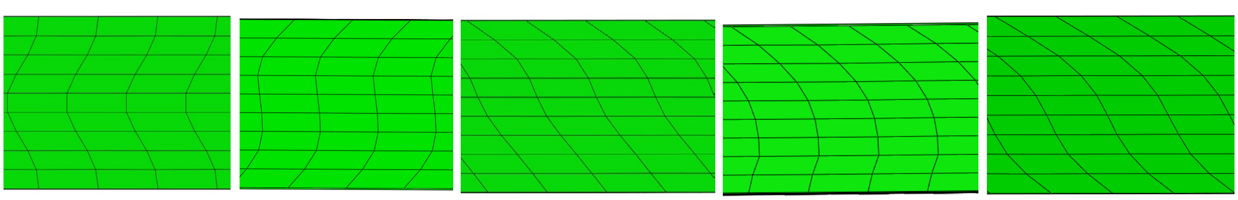

a) b) c) d) e)

Fig. 3. The deformed mesh after third pass of rolling in different variants: a) $A = 1.0$, $\alpha = 0°$, b) $A = 1.0$, $\alpha = 30°$, c) $A = 1.2$, $\alpha = 0°$, d) $A = 1.2$, $\alpha = 30°$, e) $A = 1.2$, $\alpha = -30°$.

Table 3. Stress distribution during the first rolling pass and experimental and simulated texture after sixth pass at down surface of the sample for symmetric flat and tilt rolling. The ODF cross-sections at $\varphi_2 = 0°$ are shown.

<table>
<tr><th></th><th>$A = 1.0$
$\alpha = 0°$</th><th>$A = 1.0$
$\alpha = 30°$</th></tr>
<tr><td>Normal stress components</td><td>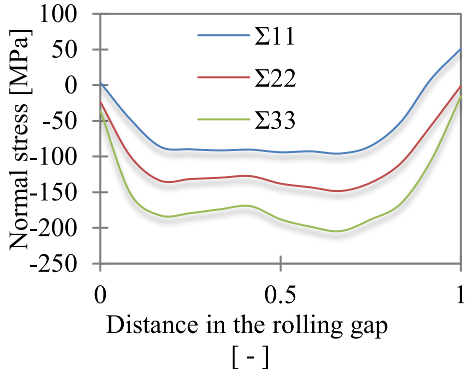
</td><td>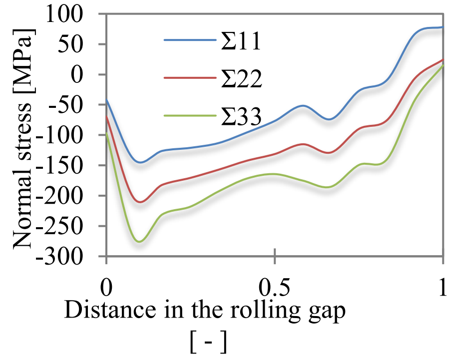
</td></tr>
<tr><td>Shear stress components</td><td>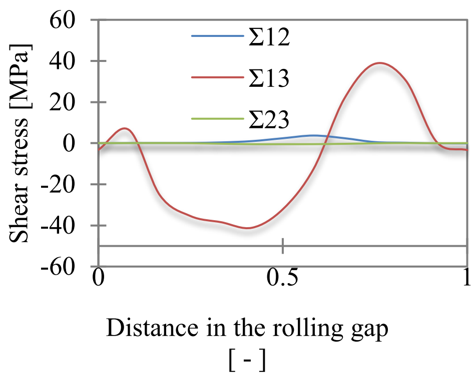
</td><td>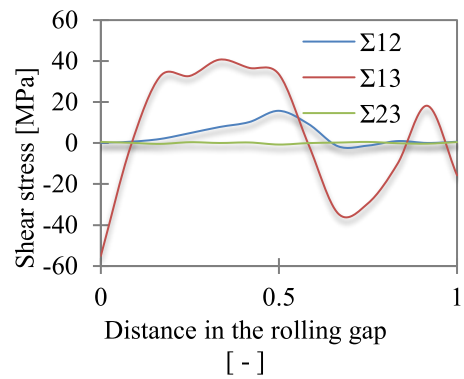
</td></tr>
<tr><td>Experimental texture</td><td>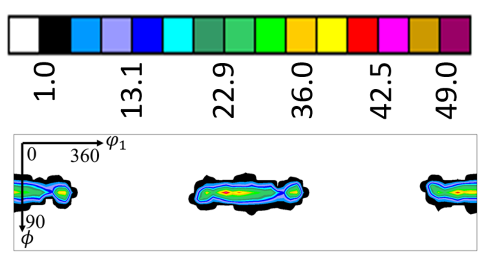
</td><td>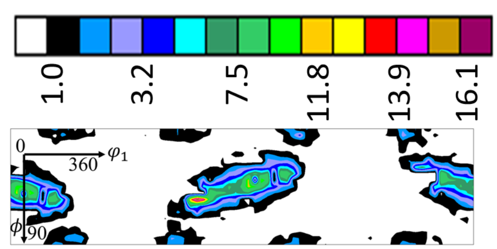
</td></tr>
<tr><td>Simulated texture</td><td>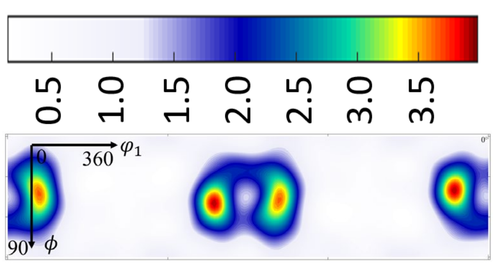
</td><td>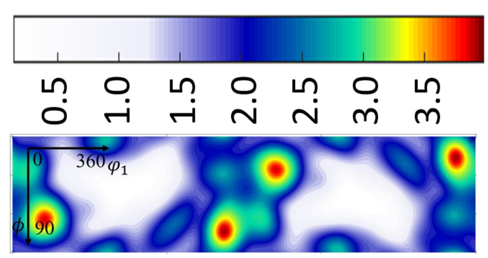
</td></tr>
</table>

Materials Research Proceedings 44 (2024) 606-614 https://doi.org/10.21741/9781644903254-65

Table 4. Stress distribution after the first pass and experimental and simulated texture after sixth pass at down surface of the sample for symmetric and asymmetric 6-pass flat rolling. The ODF cross-sections at $\varphi_2 = 0°$ are shown.

<table>
<tr><th></th><th>$A = 1.0$
$\alpha = 0°$</th><th>$A = 1.2$
$\alpha = 0°$</th></tr>
<tr><td>Normal stress components</td><td>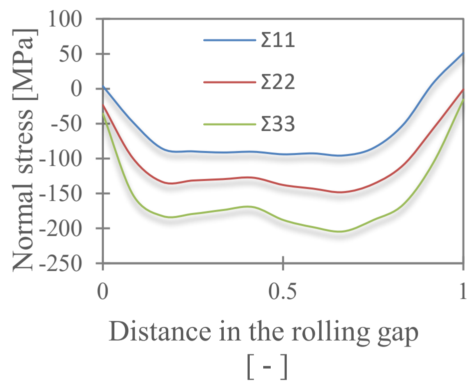
</td><td>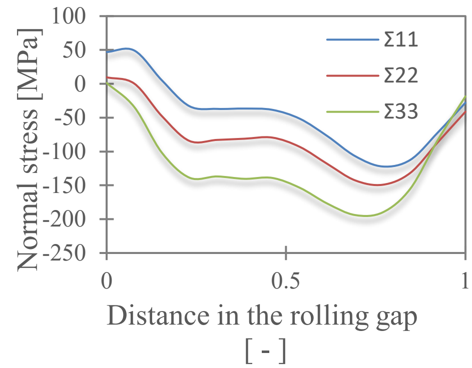
</td></tr>
<tr><td>Shear stress components</td><td>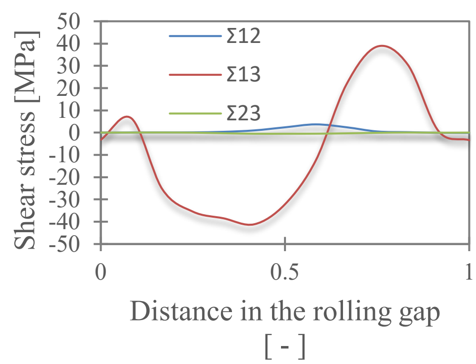
</td><td>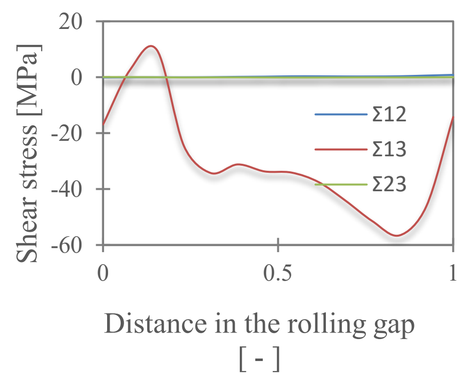
</td></tr>
<tr><td>Experimental texture</td><td>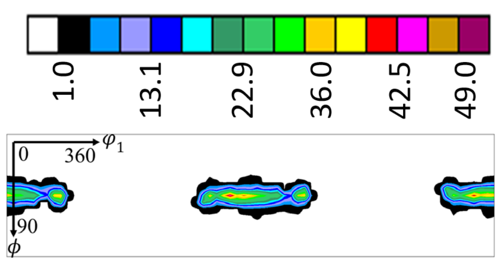
</td><td>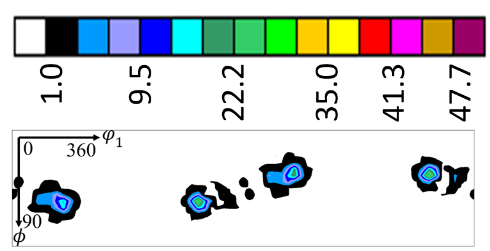
</td></tr>
<tr><td>Simulated texture</td><td>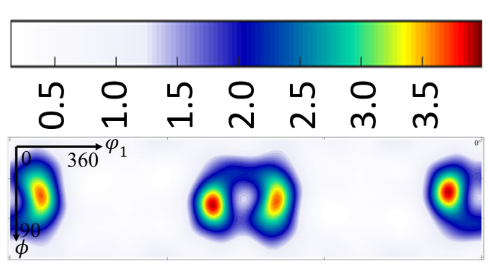
</td><td>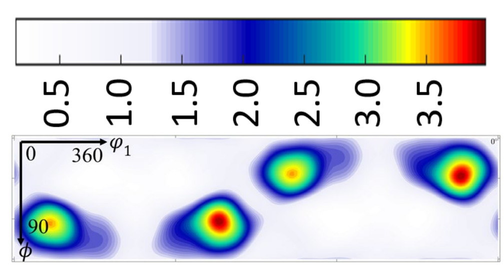
</td></tr>
</table>

It is evident that the appropriate selection of the rolling asymmetry (i.e., A and α values) can significantly homogenize the distribution of strains in the volume of the rolled flat bar.

Conclusions

The developed multi-scale model describes the evolution in the deformation field and in the crystallographic texture development of aluminum flat products. This model can be used in industry to select asymmetry conditions that enable to produce material with controlled properties through the rolled strip thickness.

Acknowledgments

We gratefully acknowledge Polish high-performance computing infrastructure PLGrid (HPC Center: ACK Cyfronet AGH) for providing computer facilities and support within computational grant no. PLG/2023/016602.

References

[1] K. Wierzbanowski, M. Wroński, T. Leffers, FCC rolling textures reviewed in the light of quantitative comparisons between simulated and experimental textures, Crit. Rev. Solid State Mater. Sci. 39 (2014) 391–422. https://doi.org/10.1080/10408436.2014.899485

[2] S. Wronski, M. Wrobel, A. Baczmanski, K. Wierzbanowski, Effects of cross-rolling on residual stress, texture and plastic anisotropy in f.c.c. and b.c.c. metals,Mater. Charact. 77 (2013) 116–126. https://doi.org/10.1016/j.matchar.2013.01.005

[3] A. Uniwersał, M. Wróbel, K. Wierzbanowski, S. Wroński, A. Baczmański, Mechanical and microstructural characteristics of polycrystalline copper rolled asymmetrically to a high deformation level, Mater. Charact. 148 (2019) 214–223. https://doi.org/10.1016/j.matchar.2018.12.017

[4] A. Uniwersał, M. Wroński, M. Wróbel, K. Wierzbanowski, A. Baczmański, Texture effects due to asymmetric rolling of polycrystalline copper, Acta Mater. 139 (2017) 30–38. https://doi.org/10.1016/j.actamat.2017.07.062

[5] M.Y. Amegadzie, D.P. Bishop, Effect of asymmetric rolling on the microstructure and mechanical properties of wrought 6061 aluminum, Mater. Today Commun. 25 (2020) 101283. https://doi.org/10.1016/j.mtcomm.2020.101283

[6] A. Uniwersał, M. Wróbel, K. Wierzbanowski, S. Wroński, M. Wroński, I. Kalemba-Rec, T. Sak, B. Bacroix, Microstructure, texture and mechanical characteristics of asymmetrically rolled polycrystalline copper, Mater. Charact. 118 (2016) 575–583. https://doi.org/10.1016/j.matchar.2016.07.004

[7] S. Wroński, K. Wierzbanowski, B. Bacroix, M. Wróbel, M. Wroński, Crystallographic textures variation in asymmetrically rolled steel, Mater. Sci. Forum 638–642 (2010) 2811–2816. https://doi.org/10.4028/www.scientific.net/MSF.638-642.2811

[8] S. Wroński, K. Wierzbanowski, B. Bacroix, T. Chauveau, M. Wróbel, Effect of asymmetric rolling on mechanical characteristics, texture and misorientations in ferritic steel, J. Cent. South Univ. 20 (2013) 1443–1455. https://doi.org/10.1007/s11771-013-1633-5

[9] H. Wang, Y. Li, G. Xu, H. Tang, Y. Wang, J. Li, B. Li, T. Zhang, W. Yu, Y. Wang, Y. Liang, The effect of asymmetric rolling on the microstructure and properties of Al–Cu–Li–TiC/TiB2 alloys, Mater. Sci. Eng. A 897 (2024) 146333. https://doi.org/10.1016/j.msea.2024.146333

[10] "United States Patent US008250895B2," Aug. 2008.

[11] A. Uniwersał, M. Wróbel, K. Wierzbanowski, S. Wroński, A. Baczmański, Rolling asymmetry effects on recrystallization process and on properties and microstructure of annealed copper, Mater. Charact. 153 (2019) 136–147. https://doi.org/10.1016/j.matchar.2019.05.001

[12] M. Wroński, K. Wierzbanowski, M. Wróbel, S. Wroński, B. Bacroix, Effect of rolling asymmetry on selected properties of grade 2 titanium sheet, Met. Mater. Int. 21 (2015) 805–814. https://doi.org/10.1007/s12540-015-5094-2

[13] K. Wierzbanowski, M. Wroński, A. Baczmański, B. Bacroix, P. Lipinski, A. Lodini, Problem of lattice rotation due to plastic deformation. Example of rolling of F.C.C materials, Arch. Metall. Mater. 56 (2011) 575–584. https://doi.org/10.2478/v10172-011-0061-5

[14] E. Schmid, W. Boas, Kristallplastizität. Springer Berlin Heidelberg, 1935.

[15] G. Wassermann, H.-J. Bunge. Mathematische Methoden der Texturanalyse Akademie-Verlag Berlin 1969, 330 Seiten Geb. M 68.–, Krist. und Tech. 5 (1970) K23–K23. https://doi.org/10.1002/crat.19700050319